Entropy analysis of frequency and shape change in horseshoe bat biosonar

Anupam K. Gupta, Dane Webster, and Rolf Müller

Entropy Analysis of Frequency and Shape Change in Horseshoe Bat Biosonar

Anupam K Gupta[a],[1] Dane Webster,[2] and Rolf Müller[1,3]

[1]*Department of Mechanical Engineering,*

Virginia Tech, Blacksburg, Virginia 24061

[2]*School of Visual Arts, Virginia Tech, Blacksburg, Virginia 24061*

[3]*Shandong University - Virginia Tech International Laboratory,*

Shandong University, Jinan 250100, China

[a] e-mail: anupamkg@vt.edu

ABSTRACT

Echolocating bats use ultrasonic pulses to collect information about their environments. Some of this information is encoded at the baffle structures – noseleaves (emission) and pinnae (reception) – that act as interfaces between the bats' biosonar systems and the external world. The baffle beampatterns encode the direction-dependent sensory information as a function of frequency and hence represent a view of the environment. To generate diverse views of the environment, the bats can vary beampatterns by changes to: 1) the wavelengths of the pulses or 2) the baffle geometries. Here, we compare the variability in sensory information encoded by just the use of frequency or baffle shape dynamics in horseshoe bats. For this, we use digital and physical prototypes of both noseleaf and pinnae. The beampatterns for all prototypes were either measured or numerically predicted. Entropy was used as a measure to compare variability as a measure of sensory information encoding capacity. It was found that new information was acquired as a result of shape dynamics. Furthermore, the overall variability available for information encoding was similar in case of frequency or shape dynamics. Thus, shape dynamics allows the horseshoe bats to generate diverse views of the environment in the absence of broadband biosonar signals.

I.. INTRODUCTION

Bats have mastered life in complex environments by relying primarily on their biosonar systems to collect sensory information about the presence, location, and nature of sound sources in the environment [1–3]. A good example of these capabilities are greater horseshoe bats (*Rhinolophous ferrumequinum*), a species that is able to navigate in dense structure-rich vegetation [4, 5] and hunt prey either in flight or by gleaning from surfaces [6, 7]. The sensory information required to accomplish this must be encoded at the interfaces of the bats' biosonar system and the external world, i.e., as the emitted sounds exit the bat's nostrils or as the returning echoes impinge on its ears. The space-frequency characteristics of the emission and reception structures can be described by a "beampattern", a scalar-valued function that specifies the output or input gain of the system as a function of spatial direction and frequency. Each beampattern can hence be seen as a space-frequency filter that provides a certain view of the environment. The ability to generate different beampatterns could help the bats to obtain different views of their environment in order to tailor the received sensory information to their current needs.

Beampatterns are the result of a diffraction process in which the outgoing or incoming ultrasonic wave packets interact with the surfaces of baffles shapes such as the noseleaves (emission) and the outer ears (reception). Hence, the beampatterns are determined by the geometry of the diffracting surface in conjunction with the wavelength of the diffracted sound. In principle, bats could utilize two different kinds of mechanisms to change their beampatterns, i.e., by virtue of: (i) changing the wavelength of their pulses or (ii) by changing the geometry of the diffracting surfaces. Bat species with broadband ultrasonic pulses (frequency-modulated or FM-bats for short [7]) should be in a good position to vary their beampattern shapes as a function of frequency. Their broad frequency bands correspond to a likewise broad range of wavelengths that can interact with the

3

baffle shapes in different ways to generate significantly different beampatterns [8, 9]. In general, beamwidth can be expected to decrease with increasing frequency resulting in a broader view of the environment at lower frequencies and a narrower for high frequencies [10–13]. In addition to the overall beamwidth, the shape of the beampatterns can depend strongly on frequency in terms of lobes of the beampattern that can appear, disappear, or change position with frequency [13, 14]. Thus, as a result of all these possible variations in the beampatterns with frequency, objects that are located at different angular positions in the environment will get illuminated by different signal spectra that could impact the information that will be encoded in the returning echoes. Echo spectra are known to encode information about the nature and location of targets [7, 12, 14–16]. As of now, there is very limited evidence that FM bats have control over the shapes that diffract their emitted pulses and the received echoes, an exception being the observation that certain FM bats (*Hypsugo bodenheimeri*) can change their emission beamwidth by varying their mouth gape [12].

Horseshoe bats (family Rhinolophidae) are so-called CF-FM bats (for constant-frequency - frequency-modulated [2]). Their biosonar calls consist of multi-harmonic signals, where each harmonic is dominated by a long narrow-band portion (CF component) that is framed by a frequency modulated (FM) component at the start and at the end [7].

However, the pulse energy in these calls tends to be concentrated in the CF component with the FM component containing either comparatively low portions of the pulse energy or even being left out completely on occasion [4, 17, 18]. In addition, all but the second harmonic in these multi-harmonic biosonar calls are also relatively weak. This restricts the ability of such bats to generate differing beampatterns due to variation of beampattern shape with frequency.

However, unlike what is currently known about FM-bats, CF-FM bats have a very conspicuous dynamic dimension associated with the baffles that surround the sites of ultrasonic emission (nose-

leaves) and reception (pinna, see Fig. 1). These baffles can undergo fast non-rigid deformations on time scales similar to the duration of individual pulse emissions and return echoes [19–21]. The deformations are a result of specific muscular action [22, 23] with deformation amplitudes significant in comparison to the wavelength used [19–21].

Some of the recent studies have shown that the deformations of the emission and reception baffles can bring about a significant change in the beampatterns (emission & reception) [13, 19, 21, 24, 27]. In addition, changes in the emission beampatterns of horseshoe bats during natural biosonar behaviors have been recently reported, though the underlying physical mechanism remains unknown [26]. Taken together, these studies suggest that dynamics is an important aspect of bat biosonar. It could be hypothesized that the function of the dynamics in the emission and reception baffle shapes of horseshoe bats is to produce a diversity in the views of the environment that bats with great biosonar bandwidth can achieve by virtue of frequency changes.

The goal of the work presented here has hence been to compare the diversity introduced into views of the environment by the use of either frequency or shape dynamics in horseshoe bats (*Rhinolophous ferrumequinum*) through an information-theoretical (entropy) analysis of the beampatterns. The analyzed beampatterns were obtained from detailed digital prototypes of the natural geometries of noseleaves [13, 24] & pinnae [21] as well as measurements using the biomimetic physical prototypes [24, 27]. These four different models were considered to ensure that the phenomena observed were robust functions of frequency or shape dynamics and not due to specific features in one of the model system that may not apply to bats and may be hard to reproduce in another experiment.
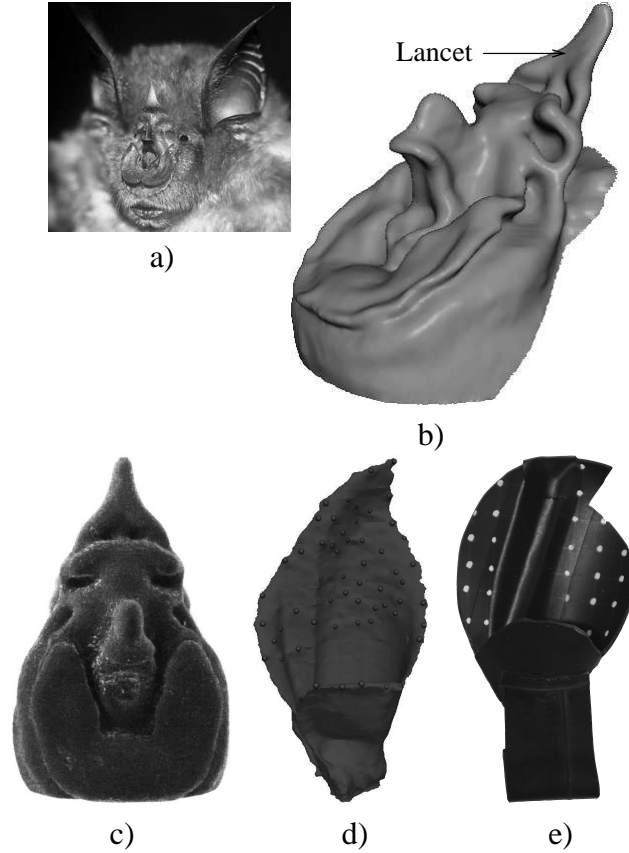
Figure 1. **Different shape sample types used to obtain acoustic far-field (beampattern) data on the noseleaf and pinna dynamics of greater horseshoe bat :** a) Portrait of a greater horseshoe bat (BP) b) Digital model used for computer animation of *in-vivo* bat noseleaf dynamics (NN), c) Exact deformable physical replica of the bat noseleaf created through 3D printing (PN, scaled $2\times$ BP) d) Digital pinna model used to recreate bat pinna dynamics (NP), e) Simplified deformable physical prototype of bat pinna (PP, scaled $2.5\times$ BP).

II.. MATERIALS AND METHODS

To obtain the shape data used in the present analysis, an adult greater horseshoe (*Rhinolophous ferrumequinum*) bat was taken from the caves in the vicinity of Jinan, Shandong Province, China

6

(latitude - $36°40'05''$ N, longitude - $116°59'49''$ E, elevation - 32 m) to serve as an experimental subject. The animal was housed in an indoor enclosure during the experiments and noseleaf and pinna motions were recorded using high-speed video cameras. In order to do the acoustic characterization of shape deformations in the study subject, four models that included both digital and physical prototypes of noseleaf and pinna were obtained. The models represented either the exact biological or biomimetic motion.

The life-like digital models were obtained from μCT scans of the noseleaf and pinna samples. In order to recreate baffle dynamics observed in high-speed video recordings of the behaving bat, different set of techniques were used for noseleaf and pinna respectively. For the noseleaf, the digital model was computer-animated using skeletal animation techniques. This involved setting up of a skeleton with control points and joints attached to the mesh such that it approximates observed noseleaf motion in bats [24] (see Figs. 1(b), 2). For the pinna, a linear elastic finite element model was used to combine the static pinna geometry with the three-dimensional time trajectories of the landmark points (marked on pinna) extracted from video recordings of the behaving bat [21] (see Fig. 1(d)). The acoustic properties (beampatterns) of the baffle shape deformations were then numerically predicted [21, 24] (see Figs. 3, 4).

Like the digital noseleaf model, the geometry for the physical noseleaf prototype came from μCT scan and was reproduced in full biological detail. The geometry was scaled to twice the size of horseshoe bat noseleaf and fabricated from an elastic material by 3D printing (Objet 3D printer). The geometry was scaled to ease handling and permit use of lower frequencies. The prototype was actuated by a simple linear actuator (Firgelli L12-1) that applied a force from behind to bend the lancet of the noseleaf forward mimicking the motion observed in bats [24](see Fig. 1(c)).

However, unlike the physical noseleaf prototype, the geometry for the physical pinna prototype

7

was a simplified version (scaled $2\times$ the horseshoe bat pinna) of the biological pinna. It was fabricated from an isobutyl rubber sheet and was actuated by a simple linear actuator (Firgelli L12-1) like the noseleaf prototype. A force was applied from the pinna backside to mimic the motion observed in bats [28] (see Fig. 1(e)).

The acoustic properties of all four models were characterized by beampatterns that were obtained either by measurement [24, 28] or numerical prediction [21, 24]. These beampatterns were acquired over a range of angles that spanned $180°$ in azimuth and $120°$ in elevation with a resolution $3°$. For all models, the beampatterns were obtained for five equidistant frequencies across bats' biosonar frequency broadcast range (60-80 kHz). The frequencies were adjusted inversely to compensate for the scaling of the respective physical models.

To compare the variability in the sensory information encoded across changes in frequency and baffle shape (diversity of views), the beampatterns were characterized by kernel density estimates (KDE) [29] of the probability density functions (PDFs) of the beampattern amplitudes. To compute the KDE estimates of the amplitude PDFs, a Gaussian kernel was used. The size (bandwidth) of the kernel was selected automatically using a plug-in type estimator [29–31]. The amplitude PDFs computed by KDE to characterize the beampattern data were as follows:

1. Two-dimensional joint amplitude PDFs combining beampatterns associated with different frequencies. One dimension of these PDFs was the beampattern amplitude at a reference frequency of 60 kHz and the other the beampattern amplitude at one of the five frequencies at which the bat's main biosonar band (60-80 kHz) was sampled. The values of the PDF were estimated for 2501 points along each dimension. Joint PDF estimates were obtained for each of the shape conformation stages in the studied sample.

8

2. Two-dimensional joint amplitude PDFs combining beampatterns associated with different shape conformation stages (see Fig. 5). One dimension of these PDFs was the beampattern amplitude associated with the upright shape change stage and the other the beampattern amplitude associated with one of the five stages in the entire shape change cycle. The values of the PDF were estimated for 2501 points along each dimension. Joint PDF estimates were obtained for each of the frequencies analyzed.

3. Five-dimensional joint amplitude PDFs where each dimension represented the beampattern amplitude for one of the five shape change stages in shape change cycle. Along each dimension the PDF values were estimated for 2501 points. A separate five-dimensional joint PDF was computed for each of the analyzed frequencies.

4. Five-dimensional joint amplitude PDFs where each dimension represented one of the five equidistant frequencies in the bat's biosonar range (60-80 kHz). Along each dimension the PDF values were estimated for 2501 points. A separate five-dimensional joint PDF was computed for each of the stages in the shape change cycle represented in the sample.

For each of the above KDE of the amplitude PDFs, differential entropy [31, 32] (Eq. 1) was computed to quantify the differences in variability in the sensory information encoded by just the use of frequency and shape change respectively. If $X_1, X_2, ..., X_n$ are a set of jointly distributed continuous random variables with joint probability density function $f(x_1, x_2, ..., x_n)$, the nonparametric estimate of joint differential entropy is given by Eq. 1.

$$\hat{h}(X_1, X_2, ..., X_n) = -\frac{1}{n} \sum ln(\hat{f}(x_1, x_2, ..., x_n)) \tag{1}$$

where $\hat{h}(X_1, X_2, ..., X_n)$ is the nonparametric estimate of joint differential entropy $h(X_1, X_2, ..., X_n)$,

9

136    $\hat{f}(x_1, x_2, ..., x_n)$ is the kernel density estimate (KDE) estimate of joint probability density function

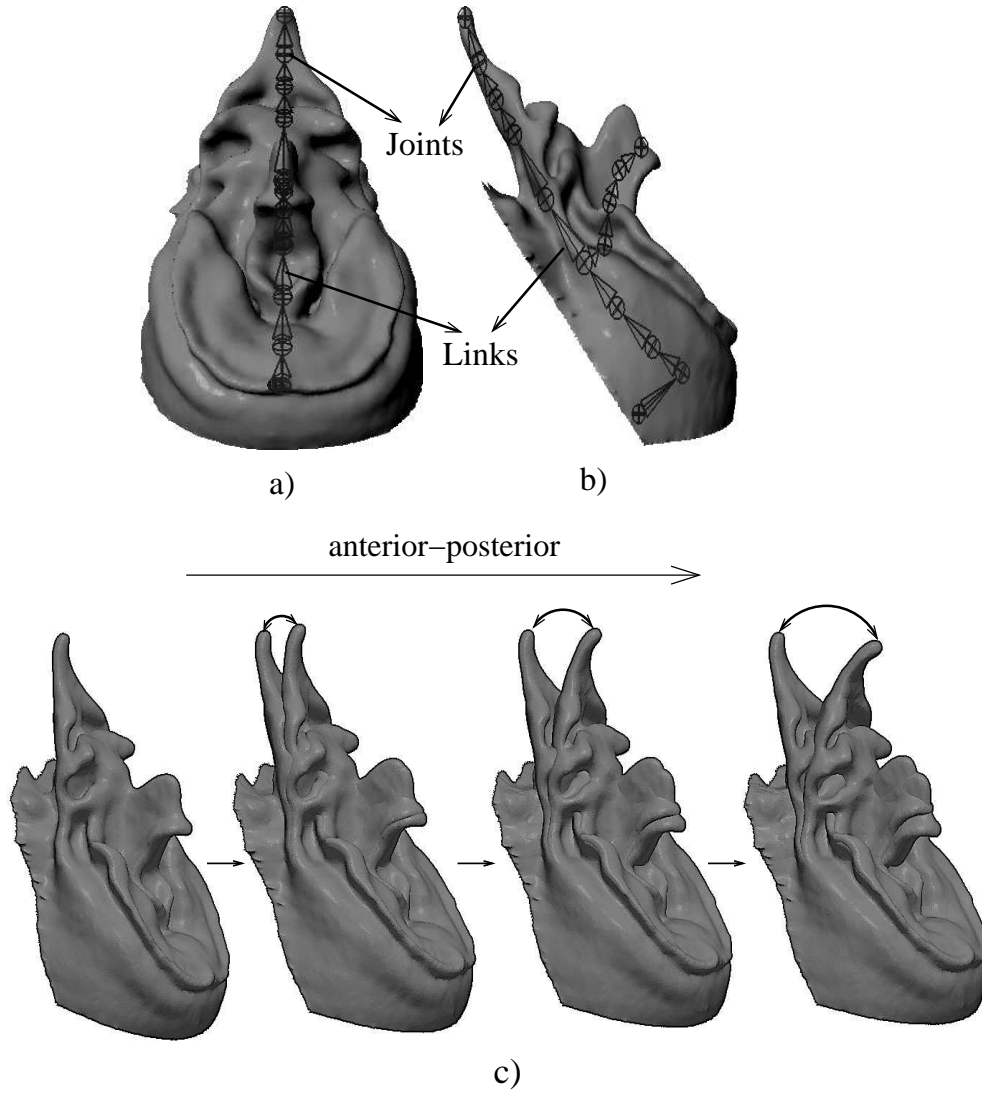137 $f(x_1, x_2, ..., x_n)$ and n is the number of samples.

Figure 2. **Digital rigged noseleaf model of greater horseshoe bat (*Rhinolophus ferrumequinum*):** a) front view, b) side view, c) Lancet anterior-posterior motion recreated in digital bat noseleaf model using skeletal animation techniques (rigging).
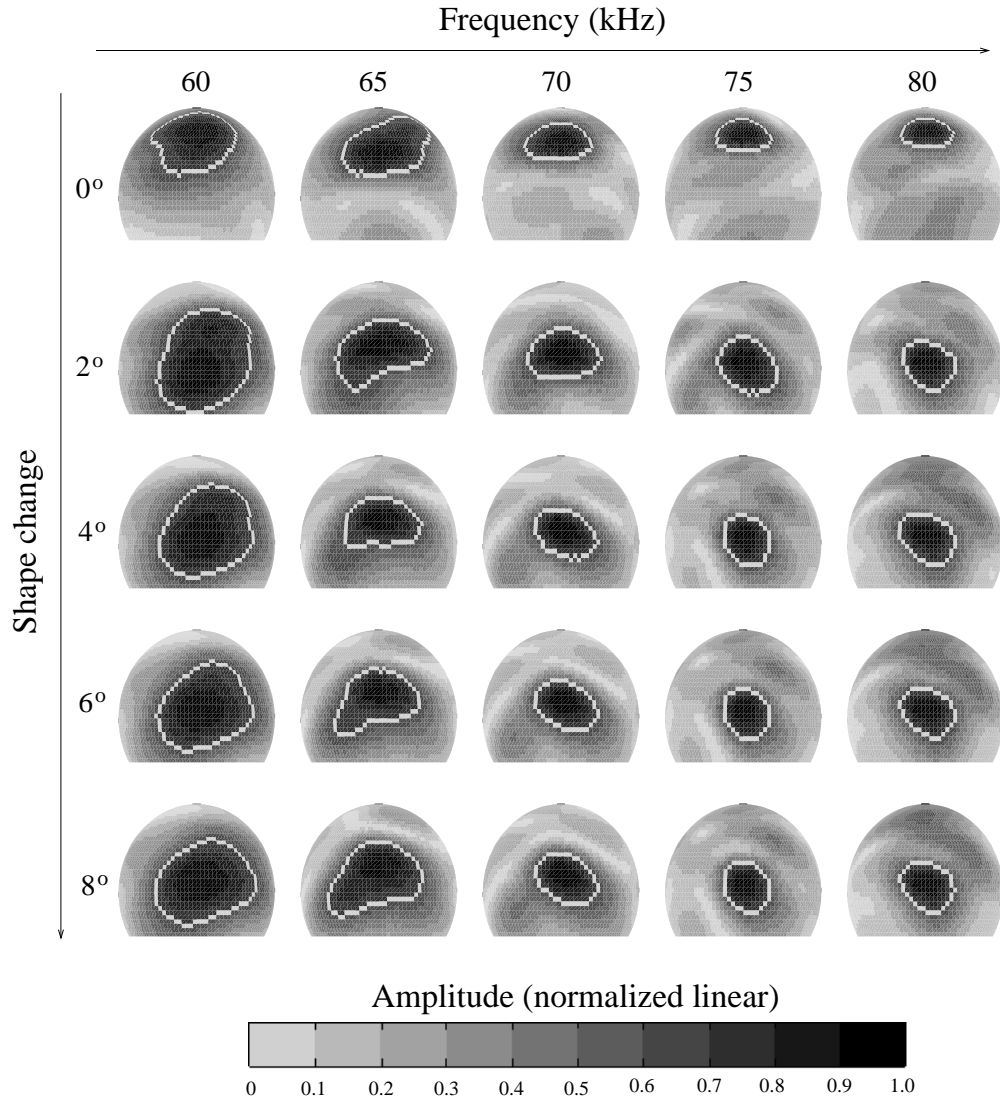
Figure 3. **Numerically predicted beampatterns for the bat noseleaf digital model.** Each row shows different lancet positions. Each column shows different frequencies. The gray-level coding is linear.
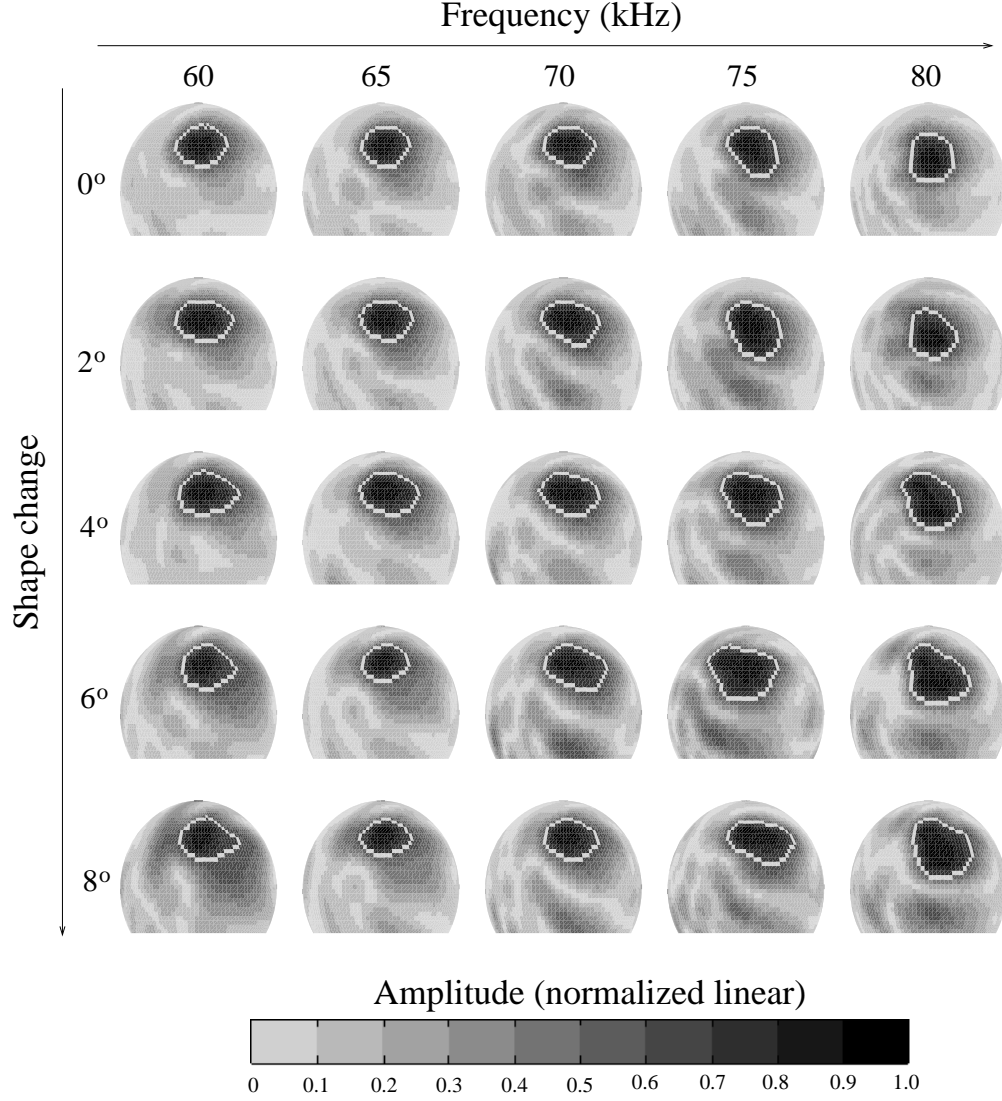
Figure 4. **Numerically predicted beampatterns for bat pinna digital model.** Each row shows different pinna positions. Each column shows different frequencies.The gray-level coding is linear.

III.. RESULTS

The joint 2D probability density functions of the normalized beampattern amplitudes across shape change stages (Fig. 5) and across frequency (Fig. 6) were both found to deviate considerably from a diagonal structure which would indicate that no additional information encoding capacity

is created by adding frequencies or shape conformations. They were also far from uniform which would maximize the joint information encoding capacity, but showed intricate patterns, i.e., the beampattern amplitudes across different frequencies or shape conformations were found to have complex statistical dependencies, evident in multiple ridges in the pdfs.

The patterns in the joint 2d pdfs differed between the shape conformations and the frequencies indicating that the statistical dependencies are not the same for changes in shape and changes in frequency.
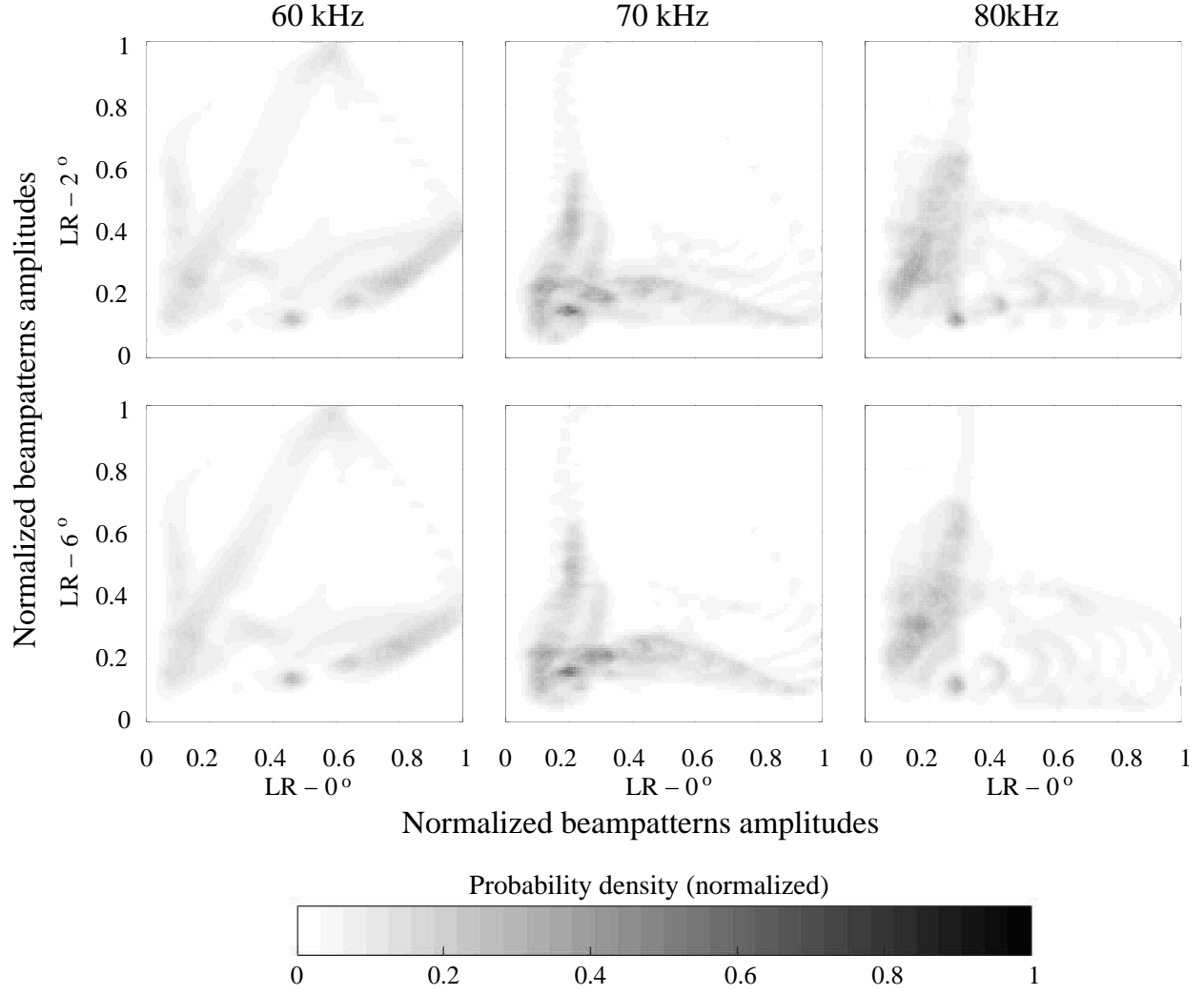
Figure 5. **Joint probability density function across lancet shape change.** The rows show the 2D joint

probability density functions between the lancet upright stage (LR - 0°) and subsequent shape change stages

i.e. LR - 2° & LR - 6° respectively, in the shape change cycle. The columns show the joint pdfs between

lancet shape change stages for multiple frequencies in bats' biosonar frequency broadcast range (60-80

kHz). Datasets used here are numerically predicted acoustic estimates for NN model. NN refers to the
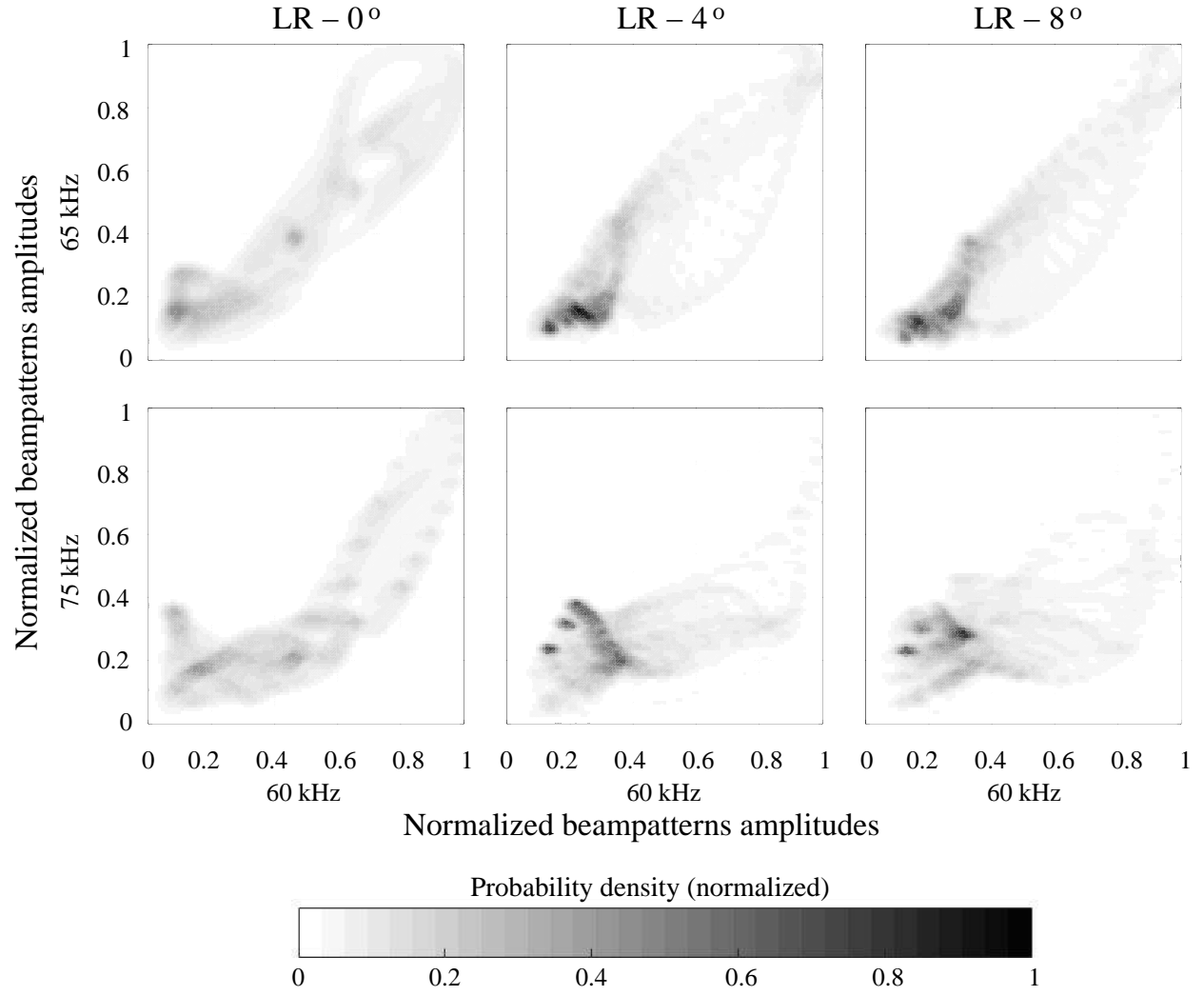
sample shown in Fig.1. LR refers to lancet rotation.

Figure 6. **Joint probability density function across frequency.** The rows show the 2D joint probability density functions between the lowest frequency (60 kHz) and subsequent frequencies, i.e. 65 kHz & 75 kHz respectively in bats' biosonar frequency broadcast range (60-80 kHz). The columns show the 2D joint pdfs between frequencies for multiple lancet shape change stages in the shape change cycle. Datasets used here are numerically predicted acoustic estimates for NN model. NN refers to the sample shown in Fig.1. LR refers to lancet rotation.

149   For changes in baffle shape, the joint entropy values estimated from the joint pdfs depended

150 on the distance between the two shape conformations that were used to compute the joint entropy

15

(Fig. 7(a)). The further a tested conformation stage was separated from the upright stage that was used as a reference, the larger the joint entropy between these two stages. With the exception of the numerical noseleaf model (NN), an average increase of one bit (approx. 21%) in joint entropy was observed between the upright stage and the farthest conformation stage across all models (Fig. 7(a)).

The joint entropy values computed by combining different frequencies did not show the same systematic dependence on distance between the compared beampatterns that was seen among the changes in shape. For the frequencies, a reference frequency of 60 kHz was compared to five frequencies spaced equally between 60 and 80 kHz. For all models, this comparison let to an average joint entropy change of 0.4 bits (approx. 12%) between the lowest and highest entropy values regardless of the spectral separation between the two frequencies (Fig. 7(b)).

To compare the variability in encoded information across all five shape conformation stages and five frequencies, five dimensional joint pdfs were estimated for both cases, i.e., across frequency and shape change. The entropy estimates for the joint pdfs across all five shape change stages and five frequencies were found to be comparable, with an average difference in entropy of 1.2 bits (approx. 8%) observed across all models (Fig. 8).

The different frequency and shape change configurations were additionally tested for a broad range of SNR (signal-to-noise-ratio) values (-50 to -15 dB) to test the dependence of observed effects on SNR. It was found that the effects of frequency and shape change were qualitatively similar across all tested SNR values.
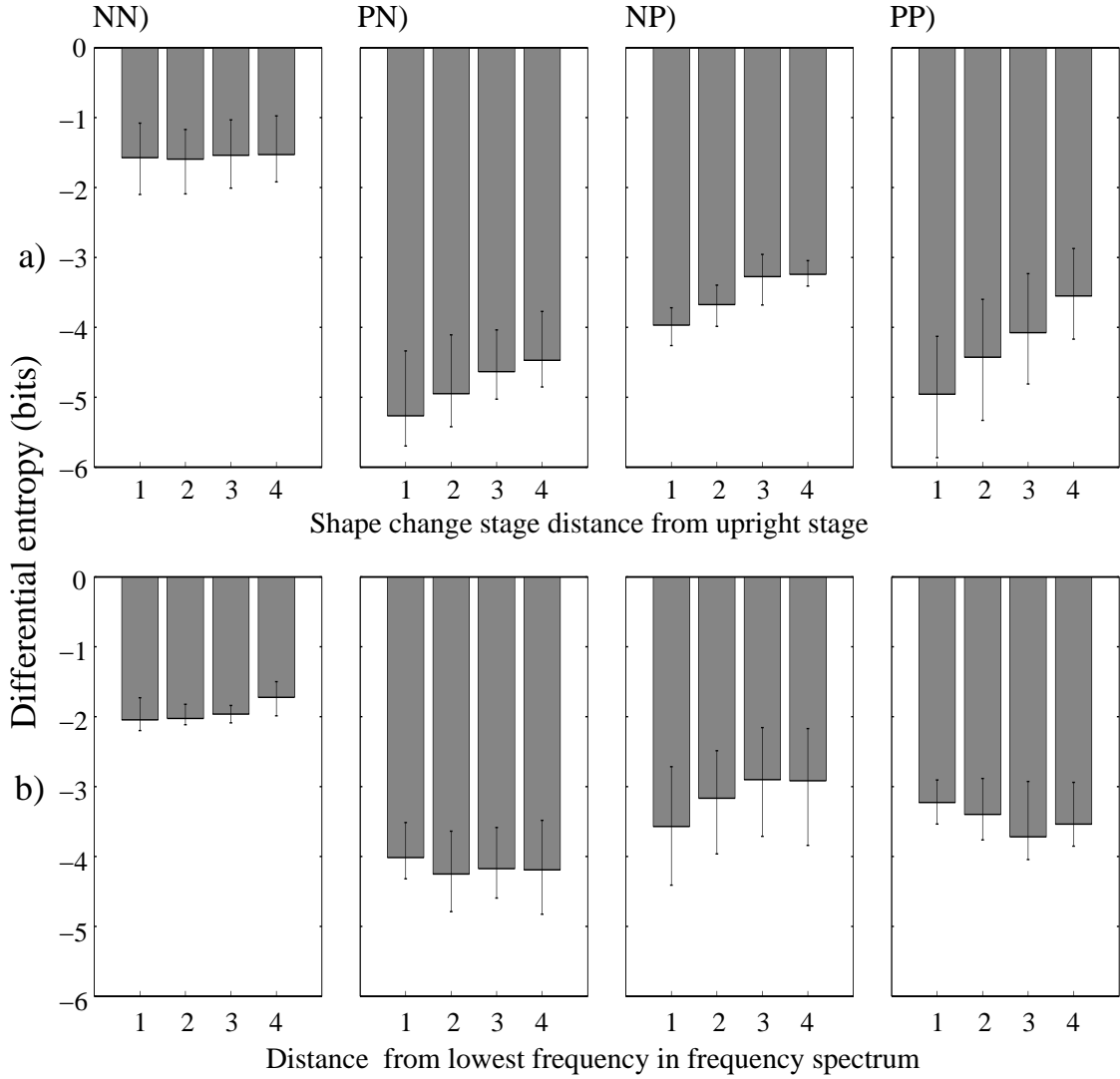
16

Figure 7. **Average joint entropy estimates in bits.** (a) From left to right, bar height represents the joint entropy estimate for a shape change stage with upright (reference) stage as a function of distance from the upright (reference) stage in shape change cycle (averaged over five equidistant frequencies between 60-80 kHz). (b) From left to right, bar height represents a joint entropy estimate for a frequency with lowest frequency (60 kHz) as a function of distance from the lowest frequency in bats' biosonar frequency broadcast range (60-80 kHz) divided into five equidistant frequencies (averaged over five stages in shape change cycle). Error bars indicate the minimum and maximum values of entropy. NN, PN, NP, PP refer to the samples shown in Fig.1.
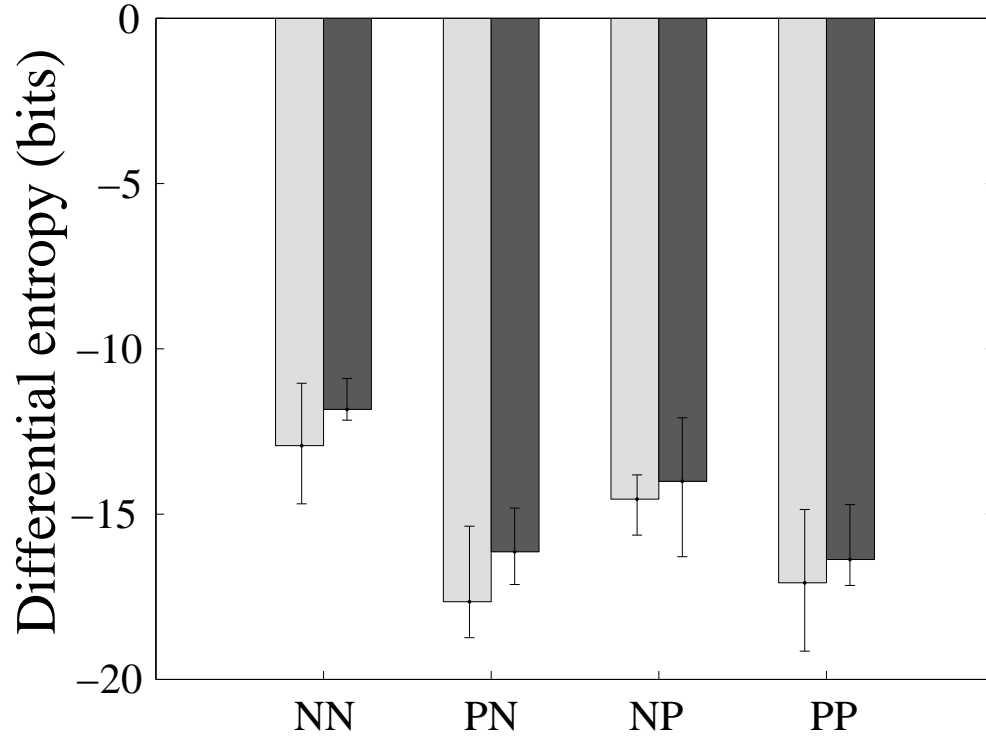
Figure 8. **Pooled average entropy estimates in bits.** Light gray bar height represents the joint entropy estimate across all the shape change stages (averaged over five equidistant frequencies between 60-80 kHz). Dark gray bar height represents the joint entropy estimate across all five equidistant frequency in bats' biosonar frequency broadcast range (60-80 kHz) (averaged over five stages in shape change cycle). Error bars indicate the minimum and maximum values of entropy. NN, PN, NP, PP refer to the samples shown in Fig.1.

IV..   DISCUSSION

In the results presented here, both shape change and frequency change were found to have an approximately equal effect on increasing the variability (entropy) of the sensory inputs.

Since the analysis presented here has been aimed at investigating the relative merit of frequency

18

and shape changes for sensory information encoding, it did not delve into how this sensory information capacity could translate into performance into any given sensory task or how far such a performance would be from an optimum solution. Since it is well established that spectral features (i.e., changes over frequency) can support source localization in bats (e.g., [33]) and shape change and frequency were found to have a similar effect on sensory information encoding capacity, it can be hypothesized that the shape changes could also support the animal's need for direction-dependent sensory information.

The joint probability density function estimates obtained here indicate that neither additional shape conformations nor additional frequencies enhances information encoding capacity in an optimum way that would be given by a uniform joint PDF. This could be due to physical constraints on changes that can be made to the shapes of a noseleaf or pinna, how much these changes can influence the beampatterns, and how different beampatterns are possible. A recent study [34] has shown that bat biosonar beampatterns are more variable than a random reference (irregular cones made from crumpled aluminum foil) in terms of beamwidth which could be seen as an indication that factors other than beamwidth have driven the evolution of these characteristics.

The only difference found between altering the beampattern based on frequency or shape change was that whereas the differential entropy values increased with the distance between different shape conformations, they remained approximately the same between frequencies, i.e., regardless of the spectral distance between these frequencies. Since the change in wavelengths (about 1.5 millimeter over the analyzed frequency band) were substantially less than the maximum displacements associated with the changes in shape (several millimeters), this cannot be explained by the amplitude of the geometrical changes. Instead, it could be hypothesized that the difference is due to the local nature of the shape changes where only certain parts of the baffle being moved

19

versus the global nature of the frequency changes where the wavelength changes affect the entire diffraction process.

The observed effects were found to be qualitatively similar across all four datasets despite the differences in either experimental approach (numerical versus physical) or biological detail reproduced (life-like versus simplified). This suggests that the results are a robust function of either overall shape dynamics or frequency and not due to methodological peculiarities as the datasets have little in common in terms of experimental protocol.

The observed similarity between the variability that has been introduced by changes in baffle shapes or frequency changes indicates that both types of changes could be equally well suited for enhancing the encoding of sensory information through the diverse sets of beampatterns they create. Hence, horseshoe bats could have two alternative mechanisms for increasing the amount of sensory information they receive via their biosonar echoes: relying on the echoes to the FM-tails of their biosonar pulses or changing the shape of their noseleaves and pinnae. The bats could use both mechanisms for pulses that contain strong FM-tails and are accompanied by noseleaf and/or pinna motions. They could rely on frequency diversity only for pulses that have strong FM-tails but are not accompanied by any dynamic shape changes changes. Finally, the bats could rely on shape diversity only in situations where the FM-tails are weak, but the CF-components of their pulses are accompanied by dynamic changes in baffle shape. Only in cases, where the bats emit pulses with a weak FM-tail and no shape changes would they be left with a minimum of monaural information related to target direction.

The need to concentrate pulse energy in a narrow frequency band for the detection of Doppler shifts could have been an evolutionary driving force behind the evolution of the noseleaf and pinna dynamics in horseshoe bats. The narrower the frequency band of the pulses, the smaller the amount

20

of monaural, direction-related sensory information that the animals have access to. Noseleaf and pinna deformation could hence be seen as evolutionary innovations to break this linkage between bandwidth and the encoding of monaural direction information. The current findings affirm the importance of biosonar dynamics in the biosonar system of horseshoe bats which is in accordance with a host of recent studies: Dynamic changes in the shape of lancet [19], anterior leaf [20] and pinnae [21] have been previously reported. These motions were found to occur on timescales of individual pulses or echoes and have been hypothesized to have an effect on encoding of sensory information [19–21]. Moreover, horseshoe bats have been shown to actively adjust beam width during terminal stages of prey capture [26]. Furthermore, the shape changes in lancet and pinnae have been previously reported to help encode additional information that significantly improves the number of resolvable directions and accuracy of direction finding in horseshoe bats [35]. The present findings give further credence to the hypothesis that dynamics plays an important role in the encoding of sensory information. The current finding is particularly interesting as it suggests that baffle shape change could be a novel way evolved by CF-FM bats to generate diverse beampatterns to tailor the biosonar view to the task at hand in the absence of broadband biosonar signals.

[1] N. Suga, "Biosonar and neural computation in bats", Scientific American **262**, 60–68 (1990).

[2] G. Neuweiler, *Biology of Bats*, chapter 6 (Oxford University Press, New York, USA) (2000).

[3] H.-U. Schnitzler and J. O.W. Henson, *Mammal Species of the World: A Taxonomic and Geographic Reference*, volume 28, chapter Performance of airborne animal sonar systems: I. Microchiroptera, 109–181 (Springer) (1980).

[4] G. Neuweiler, W. Metzner, U. Heilmann, R. Rbsamen, M. Eckrich, and H. Costa, "Foraging behaviour and echolocation in the rufous horseshoe bat (rhinolophus rouxi) of sri lanka", Behavioral Ecology and Sociobiology **20**, 53–67 (1987).

[5] G. Jones and J. Rayner, "Foraging behavior and echolocation of wild horseshoe bats rhinolophus ferrumequinum and r. hipposideros (chiroptera, rhinolophidae)", Behavioral Ecology and Sociobiology **25**, 183–191 (1989).

[6] B. Siemers and T. Ivanova, "Ground gleaning in horseshoe bats: Comparative evidence from *Rhinolophus blasii, R. euryale and R. mehelyi*", Behavioral Ecology and Sociobiology **56**, 464–471 (2004).

[7] H.-U. Schnitzler and E. K. Kalko, "Echolocation by insect-eating bats: We define four distinct functional groups of bats and find differences in signal structure that correlate with the typical echolocation tasks faced by each group", Bioscience **51**, 557–569 (2001).

[8] A. Surlykke, S. Pedersen, and L. Jakobsen, "Echolocating bats emit a highly directional sonar sound beam in the field", Proceedings of the Royal Society of London B: Biological Sciences **276**, 853–860 (2009).

[9] U. Firzlaff and G. Schuller, "Spectral directionality of the external ear of the lesser spear-nosed bat, *Phyllostomus discolor*", Hearing Research **181**, 27–39 (2003).

265 [10] G. K. Strother and M. Mogus, "Acoustical beam patterns for bats: Some theoretical considerations", The Journal of the Acoustical Society of America **48**, 1430–1432 (1970).

267 [11] L. Jakobsen, J. M. Ratcliffe, and A. Surlykke, "Convergent acoustic field of view in echolocating bats", Nature **493**, 93–96 (2013).

269 [12] G. Arditi, A. J. Weiss, and Y. Yovel, "Object localization using a biosonar beam: how opening your mouth improves localization", Royal Society Open Science **2** (2015).

271 [13] A. K. Gupta, D. Webster, and R. Müller, "Interplay of lancet furrows and shape change in the horseshoe bat noseleaf", J. Acoust. Soc. Am **138**, 3188–3194 (2015).

273 [14] R. Müller, "Numerical analysis of biosonar beamforming mechanisms and strategies in bats", J. Acoust. Soc. Am. **128**, 1414 (2010).

275 [15] R. Müller, H. Lu, and J. R. Buck, "Sound-diffracting flap in the ear of a bat generates spatial information", Phys. Rev. Lett. **100**, 108701 (2008).

277 [16] R. Müller*, A. Gupta*, H. Zhu, M. Pannala, U. Gillani, Y. Fu, P. Caspers, and J. Buck, "Dynamic hearing enhances sensory information encoding in bats", Phys. Rev. Lett. (2016), under review.

279 [17] H.-U. Schnitzler, H. Hackbarth, U. Heilmann, and H. Herbert, "Echolocation behavior of rufous horseshoe bats hunting for insects in the flycatcher-style", Journal of Comparative Physiology A **157**, 39–46 (1985).

282 [18] B. Tian and H.-U. Schnitzler, "Echolocation signals of the greater horseshoe bat (*Rhinolophus ferrumequinum*) in transfer flight and during landing", J. Acoust. Soc. Am. **101**, 2347–2364 (1997).

284 [19] W. He, S. C. Pederson, A. K. Gupta, J. A. Simmons, and R. Müller, "Lancet dynamics in greater horseshoe bats, *Rhinolophus ferrumequinum*", PloS ONE **10** (2015).

286 [20] L. Feng, L. Gao, H. Lu, and R. Müller, "Noseleaf dynamics during pulse emission in horseshoe bats", PloS ONE **7**, e34685 (2012).

[21] L. Gao, S. Balakrishnan, W. He, Z. Yan, and R. Müller, "Ear deformations give bats a physical mechanism for fast adaptation of ultrasonic beam patterns", Phys. Rev. Lett. **107**, 214301 (2011).

[22] L. Göbbel, "Morphology of the external nose in hipposideros diadema and lavia frons with comments on its diversity and and evolution among leaf-nosed microchiropters", Cells Tissues Organs **170**, 39–60 (2002).

[23] H. Schneider and F. P. M ohres, "Die ohrbewegungen der hufeisenflederm ause (chiroptera, rhinolophidae) und der mechanismus des bildh orens", J. Comp. Physiol. A **44**, 1–40 (1960).

[24] A. K. Gupta, Y. Fu, D. Webster, and R. Müller, "Bat noseleaves as an inspiration for smart emission baffle structures", in *ASME 2013 Conference on Smart Materials, Adaptive Structures and Intelligent Systems*, V002T06A010 (A.S.M.E.) (2013).

[25] M. Pannala, Z. M. Sajjad, and R. Müller, "Interplay of static and dynamic features in biomimetic smart ears", Bioinspiration & Biomimetics **8**, 026008 (2013).

[26] N. Matsuta, S. Hiryu, E. Fujioka, Y. Yamada, H. Riquimaroux, and Y. Watanabe, "Adaptive beamwidth control of echolocation sounds by cf-fm bats, rhinolophus ferrumequinum nippon, during prey-capture flight", J Exp. Biol. **216**, 1210–1218 (2013).

[27] M. Pannala, S. Z. Meymand, and R. Müller, "Interplay of static and dynamic features in biomimetic smart ears", Bioinspiration & biomimetics **8**, 026008 (2013).

[28] R. Müller, M. Pannala, O. P. K. Reddy, and S. Z. Meymand, "Design of a dynamic sensor inspired by bat ears", Smart Materials and Structures **21**, 094025 (2012).

[29] A. R. Webb and K. D. Copsey, *Statistical Pattern Recognition*, chapter 4 (John Wiley & Sons) (2011).

[30] P. Hall, S. J. Sheather, M. Jones, and J. Marron, "On optimal data-based bandwidth selection in kernel density estimation", Biometrika **78**, 263–269 (1991).

[31] A. Ihler and M. Mandel, "Kernel density estimation toolbox for matlab (R13)", `http://www.ics.uci.edu/~ihler/code/kde.html/` (2003), [Online; accessed 10-Nov-2014].

[32] I. Ahmad and P.-E. Lin, "A nonparametric estimation of the entropy for absolutely continuous distributions", Information Theory, IEEE Transactions on **22**, 372–375 (1976).

[33] J.M. Wotton and R.L. Jenison, "A backpropagation network model of the monaural localization information available in the bat", J. Acoust. Soc. Am. **101**, 2964–2972 (1997).

[34] B. Todd and R. Müller, "A Comparison of the Role of Beamwidth in Biological and Engineered Sonar", Bioinsp. Biomim. **13**, 016014 (2018).

[35] R. Müller[*], A. K. Gupta[*], H. Zhu, M. Pannala, U.S. Gillani, Y. Fu, P. Caspers and J.R. Buck, "Dynamic Substrate for the Physical Encoding of Sensory Information in Bat Biosonar", Phys. Rev. Lett. **118**, 158102 (2017), [*] **co-first authors**.